doi: 10.56761/EFRE2022.C4-P-018702

Effect of ion assistance parameters on the properties of Ir coatings

A.S. Kamenetskikh[*], *N.V. Gavrilov*

Institute of Electrophysics UB RAS, Yekaterinburg, Russia
[*]*alx@iep.uran.ru*

Abstract. Iridium coatings were deposited on Ni substrates by magnetron sputtering with ion assistance in the plasma of a low-energy electron beam. The influence of the parameters of the ion flux on the surface of the growing coating on the microstructure, the intrinsic stresses, and the adhesion of the coating is investigated. It is shown that deposition of a coating with a dense microstructure at a low homologous temperature (~0.15) is provided under the optimal ratio of the ion current density to Ir flux ~0.5 and the ion energy ~150 eV. The coatings deposited in the optimal mode are characterized by microdistortions of the crystal lattice of ~0.9% and have a predominant crystallite orientation (111), which is a favorable factor for providing corrosion protection. A low level of intrinsic stresses (~0.5 GPa) and a high adhesion strength of the coatings (the value of the critical load at nanoindentation is more than 3000 mN) have been achieved.
Keywords: Iridium coating, magnetron sputtering, ion assistance.

1. Introduction

Iridium (Ir) is characterized by a high melting point (2447 °C), low oxygen permeability (less than 10–14 g/(cm·s) at temperatures up to 2200 °C) and an oxidation rate (less than 1 μm/h at 1800 °C), chemical stability and inertia to a number of aggressive media and factors [1]. The complex of Ir properties opens up wide opportunities for the use of bulk materials and thin coatings in high-tech fields of science and technology. Such materials are used to protect rocket engine nozzles [2], in tools for the production of high-quality glasses [3], crucibles [4], heavy metal ion sensors [5], microelectronics [6, 7], medicine [8], mirrors of X-ray telescopes [9], and elements of optical systems of spacecraft [10]. Thin Ir layers are used as an effective barrier to prevent the diffusion of carbon [11] and oxygen [12].

Anticorrosive coatings are deposited on the anodes of electrolyzers that allow increasing the life of electrodes up to several years in the dialysis of marine and wastewater [13, 14]. The demand for this type of coating is increasing significantly due to the increasing market for new electrolysis plants for hydrogen production. In the period of 2012–2020, the growth of hydrogen production in the world was 5–7% per year (in physical terms), while in Russia there was a doubling of production volumes. In order to maintain the high electrochemical characteristics of the plants during operation, coatings with a dense microstructure are required, preserving the adhesive strength at thicknesses of ~1 μm or more.

Ir coatings are deposited by metal-organic chemical vapor deposition (MOCVD) [15]. The heating of the substrate above 400 °C is required in order to create dense coatings by the MOCVD method. During the decomposition of the precursor, not only Ir particles but also other components (for example, C, H) that pollute the coating [16] are released. To suppress the incorporation of impurities, oxygen is introduced into the working medium [17], which, in turn, can actively interact with the substrate and coating material at a relatively high operating temperature, which leads to a decrease in the quality of processing.

Thick dense Ir coatings (up to 10 μm) are deposited by electrolytic deposition [18]. Since high-quality coatings cannot be obtained from aqueous solutions, one has to use unstable and toxic melts of salts [19], which significantly limits the technological capabilities of the method.

Coatings with the highest uniformity and purity are deposited by atomic layer deposition. Due to the low growth rate (less than 100 nm/h) [20], the method is used to obtain coatings of nanoscale thickness, the application of which for corrosion protection is ineffective.

Physical vapor deposition (PVD) methods, including double-discharge plasma deposition [21], magnetron sputtering in radio-frequency discharge [3, 22], and direct-current discharge [23] are used for deposition of Ir coatings most widely to date. For stable operation of deposition facility in a double-discharge plasma, it is necessary to set a relatively high negative potential not only of the sputtered Ir cathode (typical values are 800–900 V) but also of the substrates (300–400 V) [21, 24]. The energy of ions bombarding the coating in such devices is usually determined by the conditions of stable discharge combustion, and the value of the ion current density directly depends on other operating parameters (electrode potentials, gas pressure). Intense ion assistance heats the processed samples up to 800 °C, which allows to obtain dense coatings, but limits the range of substrate materials and induces significant internal stresses. The method does not make it possible to independently adjust the parameters of the ion flux on the surface of the growing coating and to determine their optimal values.

The ion energy can be regulated in a wide range when coatings deposited in high-frequency magnetron sputtering systems. At the same time, the values of the sputtered atom flux density and the ion current density are determined by the discharge power and the possibility of their separate adjustment is very limited [25]. Therefore the formation of a dense microstructure of coatings is achieved by increasing the temperature of the substrates [26]. In the case of Ir, the homologous temperature at which dense coatings are deposited (~0.3–0.5 [27]) is achieved at heating more than 700 °C, which leads to a significant increase in thermally stimulated stresses in contact with the material of the oxygen electrode of the electrolysis cell (for Ni substrate up to 4 GPa). Thus, despite significant progress, the task of obtaining corrosion-resistant Ir coatings with maintaining a low level of intrinsic stresses by PVD methods does not lose its relevance.

This study was aimed at determining the optimal conditions for deposition of Ir coatings on Ni samples of the oxygen electrode of an electrolysis cell by magnetron sputtering. In order to determine the optimal parameters of the ion flux, a plasma generator based on an electron source with a mesh plasma cathode was used in conjunction with a magnetron sputtering system [28]. This solution allows independently adjusting the main operating parameters: the flow density of sputtered atoms, the current density and ion energy, the pressure and composition of the gas, and deposits coatings with the required structural and phase state, microstructure, and physical properties. The paper presents a comprehensive study of the effect of deposition conditions on the structure and properties of Ir coating.

2. Experimental methods

Planar balanced magnetrons with a target diameter of 75 mm, which operated in a pulse-periodic mode (50 kHz, 10 μs), were used for coating deposition. The magnetrons were located on the side surface of a cylindrical vacuum chamber with an internal diameter of 300 mm. Disks with a thickness of 4 mm and mass fraction of Ir of 99.97% were used as a sputtered target. The distance between the target plane and the coated samples was 6 cm. The coating substrates were made of nickel tape of type DPRNT 0.15x200 NA NP2. The Ir deposition rate was 3.2 μm/h. The strength of the adhesive bond between the coating and the substrate was increased by the 200-nm-thick Ti sublayer applied by magnetron sputtering of a target made of titan type VT1-0 (the mass fraction of Ti is 99.7%).

A spatially homogeneous plasma was generated in the volume of the working chamber for ion assistance of the coating deposition process. A wide (80 cm^2 cross-section) beam of low-energy (100 eV) electrons was injected into the chamber for this purpose. By changing the beam current in the range of 0–12 A, the density of the ion current from the plasma was adjusted from 0.1 to 1 mA/cm^2. The ion energy was regulated independently by changing the potential of the samples in the range of 50–500 V.

The samples were cleaned in an ultrasonic bath in acetone before coating deposition, then placed in a vacuum chamber, which was pumped out by a turbomolecular pump to a pressure of $4 \cdot 10^{-3}$ Pa, and the samples were ion sputtered at a current density of 0.5 mA/cm^2 and ion energy of 500 eV for 10 min. Then the Ti sublayer and Ir coating were deposited. The Ar pressure in the experiments was 0.17 Pa. The temperature of the samples at all stages of processing did not exceed 300 °C.

X-ray phase analysis was performed on a diffractometer D8 DISCOVER (Bruker) using CuKα radiation (λ = 1.542 Å) with a graphite monochromator on a diffracted beam. The processing was performed using the full-profile analysis program TOPAS 3. Texture coefficients were determined by the technique [29]. The level of intrinsic stresses in the coatings was determined by the bending of nickel strips with a thickness of 50 μm using the Stony method [30]. The microstructure of the coatings was studied using a scanning electron microscope Merlin (Carl Zeiss NTS). The strength of the adhesive bond between the coating and the substrate was determined by scratching on Nanotest 600 (Micromaterials Ltd.) using a conical diamond indenter with a rounding radius of 5 μm. The indenter moved along the surface of the coating at a constant speed of 5 μm/s and a normal load increasing at a speed of 20 mN/s. When moving the indenter, the depth of indentation and the level of acoustic emission were measured. Their changes were used to determine the adhesion violation.

3. Results and discussion

The image of a brittle cleavage of the coating deposited at a current density (j_i) of 0.1 mA/cm2 and at ion energy of 100 eV is shown in Fig.1a. A dense coating with a thickness of ~1 μm consists of fine-grained crystallites that form elongated agglomerates with a width of ~100–200 nm and a longitudinal size comparable to the thickness of the coating. It is possible to distinguish areas of transverse destruction of agglomerates on the cleavage at an arbitrary distance from the boundary with the sublayer. For a qualitative assessment, an extended diagram of the Thornton structural zones was used [27], according to which the microstructure of the resulting coating corresponds to the transition region between zone *T* (consisting of tightly adjacent fibers) and zone 2 (dense columnar structure). Under experimental conditions, the reduced energy E^* per coating atom, defined as the product $E \cdot j_i / j_a$ (where E is the ion energy, j_a is the atomic flux density), was ~10 eV, which allowed the formation of such a microstructure at a low homological temperature (~0.15).

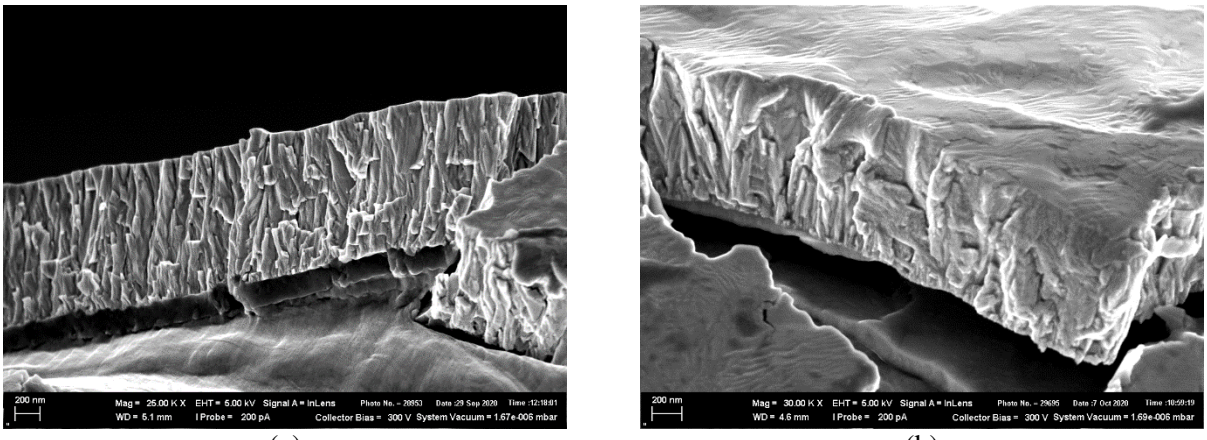

(a) (b)

Fig.1. SEM image of the transverse cleavage of the coating deposited under ion current density of 0.1 (a) and 0.5 mA/cm^2 (b). Ion energy of 100 eV.

With an increase in j_i to 0.5 mA/cm^2 (j_i/j_a ~ 0.5), the tendency to form elongated agglomerates in the direction of the coating surface is disrupted when reaching a height of several hundred nm (Fig.1b). The transverse dimensions of the crystallites increase significantly, while keeping the close contact between individual crystallites. In the thin section image (Fig.2), it is not possible to distinguish individual structural elements in the coating volume, despite the fact that the grain structure of the substrate is clearly distinguishable. There is no through porosity in the coating. The transitions between the substrate, sublayer, and coating materials are free of defects.

The transverse size of the structural formations in the coating increases with an increase in the ion current density to 1 mA/cm^2 (j_i/j_a ~ 1) and can reach values comparable to the coating thickness (Fig.3). The microstructure of the coatings corresponds to zone 3. The recrystallization of the structural elements of the coating is accompanied by the appearance of faces along the planes with minimal surface energy. In this case, as was shown in [31], large pores and cracks can occur along the boundaries of the crystallites, which significantly impairs the corrosion protection of the coatings. It can be concluded that the optimal ratio is j_i/j_a ~ 0.5 for deposition of protective Ir coating at a homologous temperature of ~0.15 and an ion energy of ~100 eV.

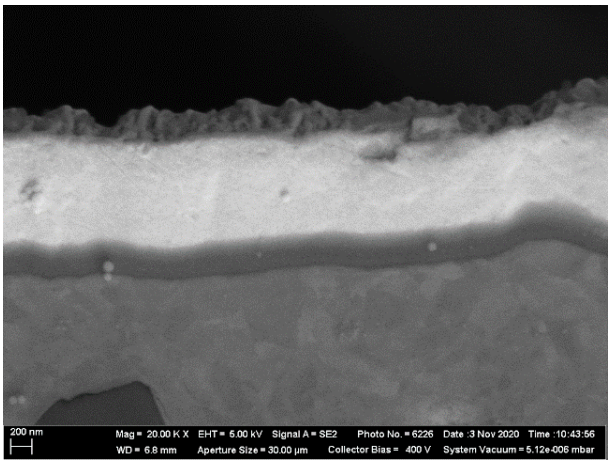

Fig.2. SEM image of the coating thin section. Ion current density of 0.5 mA/cm^2.

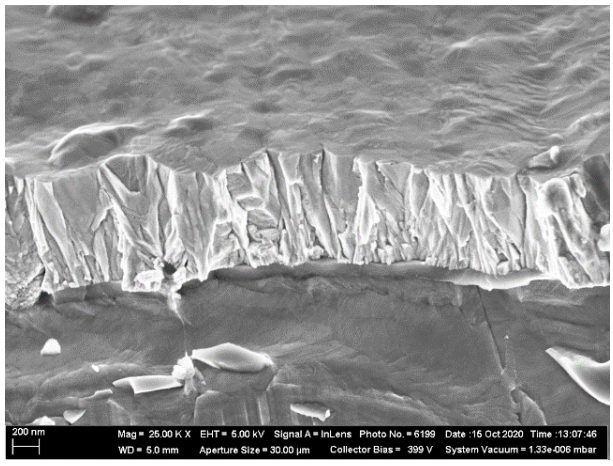

Fig.3. SEM image of the transverse cleavage of the coating deposited under ion current density of 1 mA/cm^2.

The images of brittle chips of coatings deposited with a change in E in the range of 50–200 eV and a constant j_i = 0.5 mA/cm^2 were shown in Fig.4. With an increase in energy from 50 to 100 eV, the microstructure of the coating changes from columnar (Fig.4a) to densely packed coarse-grained (Fig.2b), which is formed at the boundary of zones 2 and 3 of the Thornton diagram [27]. A further increase in the ion energy is accompanied by a decrease in the transverse dimensions of the structural elements (Fig.4b–4c). The nature of their growth becomes more orderly. A dense microstructure is preserved over the entire range of ion energy changes.

A typical X-ray diffraction pattern of the coating is shown in Fig.5. The coatings have a polycrystalline structure with a predominant crystallite orientation (111) (2θ ~ 40.7º), which is preserved over the entire ion energy range. The texture coefficient $TC_{(111)}$ reaches 3.8 at an ion energy of 50 eV, which is significantly higher than for the samples synthesized under equilibrium conditions (T = 1). An increase in the ion energy to 200 eV is accompanied by a monotonic decrease in $TC_{(111)}$ to 2.8 (Fig.6).

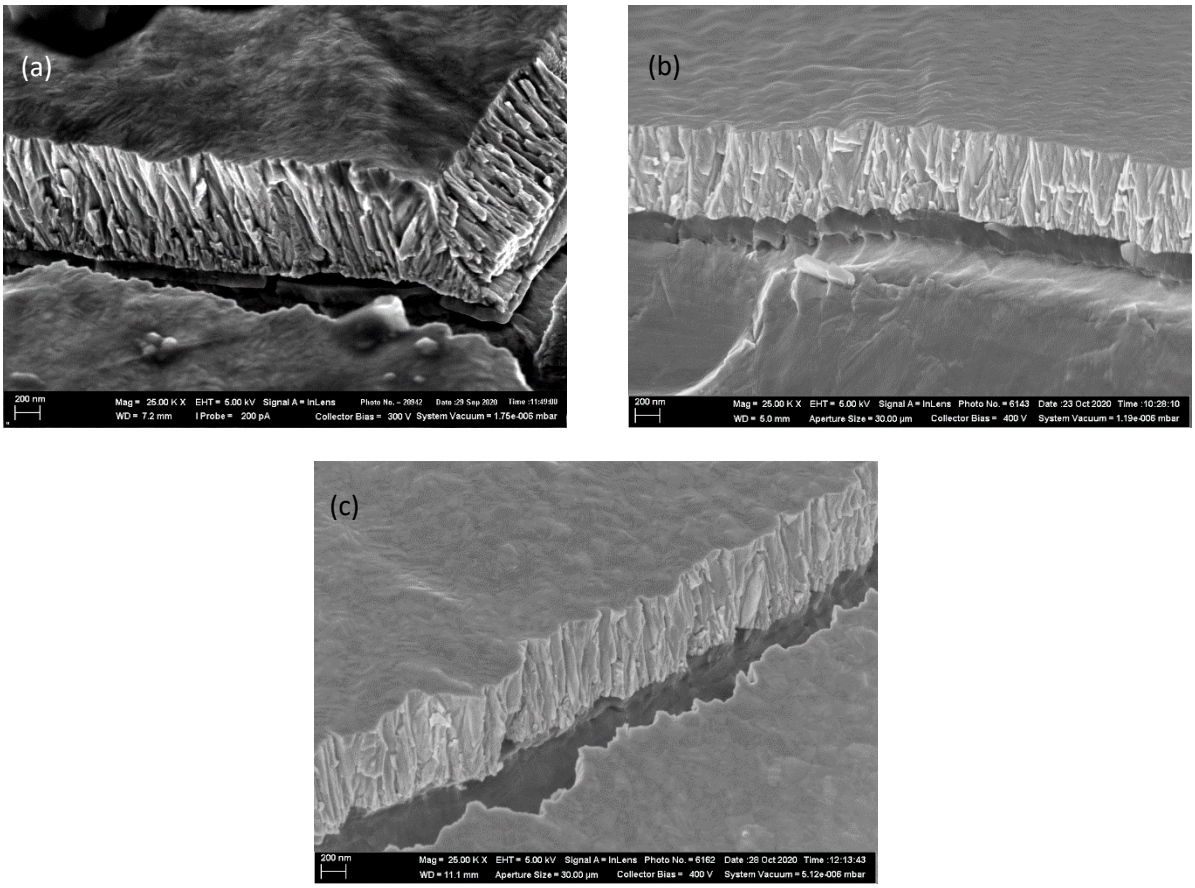

Fig.4. SEM image of the transverse cleavage of the coating deposited under ion energy of 50 (a), 150 (b) and 200 eV (c). Ion current density 0.5 mA/cm^2.

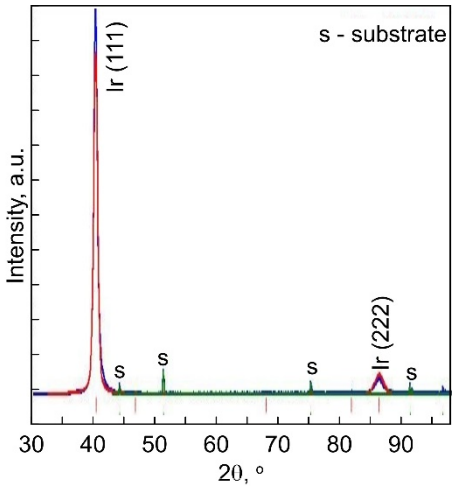

Fig.5. XRD pattern of the Ir coating.

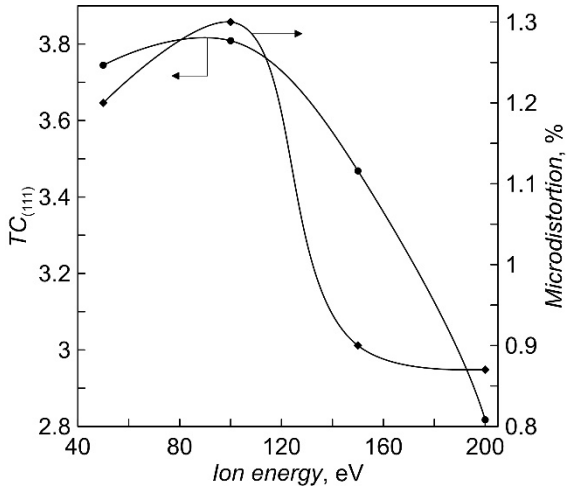

Fig.6. The Ir coating $TC_{(111)}$ and microdistortion as function of ion energy.

The results of measuring the intrinsic stresses in the coatings are shown in Fig.7. The stress level in the coatings deposited at E = 50 eV reaches 6 GPa and decreases to a minimum value of ~0.5 GPa at E = 150 eV. Since a further increase in E does not lead to a significant change in the intrinsic stresses and microdistortions of the crystal lattice, but is accompanied by a decrease in $T_{(111)}$ (Fig.6) and the growth rate of the coating and, accordingly, an increase in the consumption of

the magnetron target material, it was concluded that it was advisable to limit the value of *E* at the level of 150 eV.

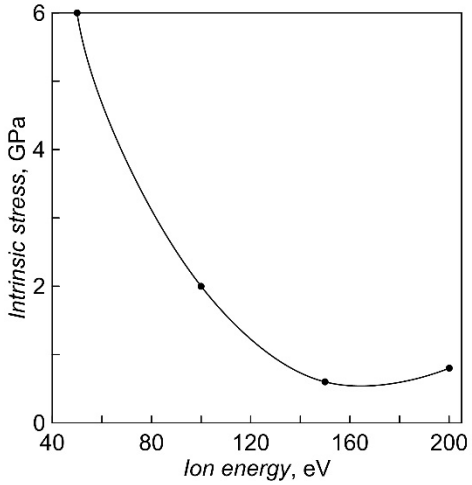

Fig.7. The intrinsic stresses in the Ir coating as function of ion energy.

Isolated cases of cracking of the coating in the direction parallel to the surface of the substrates without breaking the adhesion at loads on the indenter up to 3000 mN were observed when conducting adhesion tests of coatings with a thickness of 1 μm with a low level of intrinsic stresses. At loads of more than 3500 mN, the indenter reached the surface of the substrate, the expansion of individual folds was accompanied by a lateral breakaway of the coating. The low level of acoustic emission in the entire load range and the nature of the destruction of coatings by the type of longitudinal deformation ("buckling") [34] indicate a high adhesive strength.

4. Conclusion

The influence of ion flux parameters on the structure and properties of Ir coatings deposited by magnetron sputtering on Ni substrates at a reduced homological temperature (~0.15) was studied. It is shown that coatings with a dense microstructure corresponding to the transition zone T of the Thornton diagram and the predominant orientation of the crystallites (111) are formed at a ratio of ion/atom flux densities of ~0.5. The minimum value of the intrinsic stress (~0.5 GPa) is achieved when the ion energy increases to 150 eV. The destruction of coatings by the type of longitudinal deformation is observed at loads on the indenter of more than 3500 mN. The coatings were deposited on the surface of the electrolyzer oxygen electrode at the optimal parameters of the ion flux. According to the test results, Ir coatings reduce the rate of corrosion processes on the electrode surface by ~25%.

5. References

[1] Wu P., Chen Z., *Johnson Matthey Technol. Rev.,* **61**(1), 16, 2017; doi: 10.1595/205651317X693606
[2] Liu H., Asta M., Walle A., *Scr. Mater.*, **189**, 16, 2020; doi: 10.1016/j.scriptamat.2020.07.050
[3] Hagen J., Burmeister F., Fromm A., Manns P., Kleer G., *Plasma Process. Polym.,* **6**, S678, 2009; doi: 10.1002/ppap.200931701
[4] Merker J., Fischer B., Lupton D.F., Witte J., *Mater. Sci. Forum,* **539-543**, 2216, 2007; doi:10.4028/www.scientific.net/MSF.539-543.2216
[5] Kovacs G.T.A., Storment C.W., Kounaves S.P., *Sens. Actuators B*, **23**, 41, 1995;

doi: 10.1016/0925-4005(94)01523-K
[6] Gelfond N.V., Igumenov I.K., Boronin A.I., Bukhtiyarov V.I., Smirnov M.Yu., Prosvirin I.P., Kwon R.I., *Surf. Sci.,* **275**, 323, 1992; doi: 10.1016/0039-6028(92)90804-F
[7] Zhang W., Vargas R., Goto T., Someno Y., Hirai T., *Appl. Phys. Lett*., **64**, 1359, 1994; doi: 10.1063/1.111934
[8] Vikulova E.S., Kal'nyi D.B., Shubin Y.V., Kokovkin V.V., Morozova N.B., Hassan A., Basova T.V., *Appl. Surf. Sci.,* **425**, 1052, 2017; doi: 10.1016/j.apsusc.2017.07.100
[9] Ames A., Brunia R., Cotroneo V., *Proc. of SPIE*, **9603**, 96031I, 2015; doi:10.1117/12.2191404
[10] Yan L., Woollam J., *J. Vac. Sci. Technol. A*, **22**, 2177, 2004; doi: 10.1116/1.1781182
[11] Mumtaz K., Echigoya J., Hirai T., Shindo Y., *Mater. Sci. Engin.,* **A167**, 187, 1993; doi: 10.1016/0921-5093(93)90353-G
[12] Goswami J., Wang C., Majhi P., Shin Y., Dey A. K., *J. Mater. Res.,* **16**(8), 2192, 2001; doi: 10.1557/JMR.2001.0300
[13] Igumenov I.K., et al., *Desalination*, **136**, 273, 2001; doi: 10.1016/S0011-9164(01)00190-4
[14] Bessergenev V.G., Gelfond N.V., Igumenov I.K., *Supercond. Sci. Technol.,* **4**, 273, 1991; doi: 10.1088/0953-2048/4/7/001
[15] Hua Y., Zhang L., Cheng L., Yang W., *Mater. Sci. Engin. B*, **121**, 156, 2005; doi:10.1016/j.mseb.2005.03.020
[16] Maury F., Senocq F., *Surf. Coat. Technol*., **163–164**, 208, 2003; doi: 10.1016/S0257-8972(02)00485-1
[17] Sun Y.M., Endle J.P., Smith K., Whaley S., Mahaffy R., Ekerdt J.G., While J.M., Hance R.L., *Thin Solid Films,* **346**, 100, 1999; doi: 10.1016/S0040-6090(98)01458-8
[18] Etenko A., McKechnie T., Shchetkovskiy A., Smirniv A., *ECS Transactions*., **3**(14), 151, 2007; doi: 10.1149/1.2721466
[19] Harding W.B., *Plat. Surf. Finish.*, **65**, 30, 1978;
[20] Hamalainen J., Ritalka M., Leskela M., *Chem. Mater.,* **26**, 786, 2013; doi: 10.1021/cm402221y
[21] Zhang Z., Xu Z., Wang J., Wu W., Chen Z., *JMEPEG,* **21**, 2085, 2012; doi: 10.1007/s11665-012-0133-3
[22] Wu F., Chen W., Duh J., Tsai Y., Chen Y., *Surf. Coat. Technol.,* **163–164**, 227, 2003; doi:10.1595/205651317x693606
[23] Xin W., Peng Y., Jihong D., Zhengxian L., Yong T., Tao Y., *Rare Metal Mat. Eng.,* **45**(11), 2768, 2016; doi: 10.1016/S1875-5372(17)30037-1
[24] Wu W., Chen Z., Lin X., *Adv. Mat. Res.,* **189-193**, 688, 2011; doi: 10.4028/www.scientific.net/AMR.189-193.688
[25] El Khakani M. A., Chaker M., Le Drogoff B., *J. Vac. Sci. Technol. A*, **16**, 885, 1998; doi: 10.1116/1.581029
[26] Echigoya J., Mumtaz K., Hayasaka Y., Aoyagi E., *J. Mater. Sci.,* **39**, 6215, 2004; doi: 10.1023/B:JMSC.0000043589.23138.b6
[27] Anders A., *Thin Solid Films,* **518**, 4087, 2010; doi:10.1016/j.tsf.2009.10.145
[28] Gavrilov N.V., Kamenetskikh A.S., Men'shakov A.I., Bureyev O.A., *J. Phys.: Conf. Ser.*, **652**, 012024, 2015; doi:10.1088/1742-6596/652/1/012024
[29] Harris G.B.X., *Philos.l Mag. Ser.,* **43**(336), 113, 1952;
[30] Janssen G.C.A.M., Abdall M.M., Keulen F., Pujada B.R., Venrooy B., *Thin Solid Films,* **517**, 1858, 2009; doi: 10.1016/j.tsf.2008.07.014
[31] Huang Y., Bai S., Ye Y., *Int. J. Refract. Met. Hard Mater.*, **50**, 204, 2015; doi: 10.1016/j.ijrmhm.2015.01.009

[32] Quaeyhaegens C., Knuyt G., D`Haen J., Stals L. M., *Thin Solid Films*, **258**, 170, 1995; doi: 10.1016/0040-6090(94)06355-9
[33] Wessling B., Mokwa W., Schnakenberg U., *J. Electrochem. Soc.,* **155**(5), F61, 2008; doi: 10.1149/1.2844805
[34] Bull S.J., *Tribol. Int.,* **30**(7), 491, 1997; doi: 10.1016/S0301-679X(97)00012-1